Article:
Takahashi, S., Yamakita, S., Muto, S. et al. (10 more authors) (2025) Oceanic anoxia in Panthalassa during the Early Triassic Smithian–Spathian transition. Palaeogeography, Palaeoclimatology, Palaeoecology, 675. 113080. ISSN: 0031-0182

https://doi.org/10.1016/j.palaeo.2025.113080

Review of the stratigraphic framework of the Momotaro-Jinja section (deep-sea Lower Triassic, Japan)

The Momotaro-Jinja section consisting of the MjL and MjU sections is observed at the outcrop of pelagic deep-sea sediments (siliceous claystone and chert), which is exposed in the area next to Momotaro Park on the eastern bank of the Kiso River (Figs. 2, 3). The MjL section is composed of grey claystone and black claystone from south to north (the former is classified into gray siliceous claystone and grey cherty claystone in the present study). The MjU section is composed of grey claystone, red claystone and grey claystone with chert interbeds from south to north. Previous studies have worked on lithostratigraphy (Sakuma et al., 2012), conodont biostratigraphy (Takahashi et al., 2009; Yamakita et al., 2010, 2016) and radiolarian biostratigraphy (Sugiyama, 1997; Yao and Kuwahara, 1997) of this section. While these works generally agree on the stratigraphy of the MjU section, the MjL section has been a target of controversy. However, this controversy has not been explained in detail in published papers. Below is a review of the stratigraphy of the MjL and MjU sections.

The first work on stratigraphy of the MjL section (Yao and Kuwahara, 1997) was on radiolarian biostratigraphy. They correlated the section to the "Lower Triassic" *Parentactinia nakatsugawaensis* Zone except for the uppermost part of the MjU section, which they assigned to the "lower Middle Triassic" *Hozmadia gifuensis* Zone. This age was mostly supported by Sugiyama (1997), who studied a lateral extension of the section (Section T therein) and correlated the entire interval to the Lower Triassic. These works considered that the stratigraphic way up was to the north in both the MjL and MjU sections, consistent with the geological structure of the entire Inuyama area (Fig. 2). While radiolarian assemblages implied that the MjL section was older than the MjU section, temporal resolution was not high enough to imply the stratigraphic way up within the MjL section. Subsequently, the finding of conodonts indicated that the MjL section is correlated to the Smithian (Yamakita et al., 2010) and the MjU section is correlated to the Spathian (Takahashi et al., 2009), confirming the studies on radiolarians. The conodonts reported by Yamakita et al. (2010) also provided evidence for the northward way up of the sections.

Contrary to the above, Sakuma et al. (2012) argued that sedimentological microstructures (detailed below) indicated a general southward way up for the MjL

section. Sakuma et al. (2012) further claimed that the southern part of the MjL section included the same black claystone "key beds" as the southern part of the MjU section. Since the MjU section contains Spathian conodonts (Takahashi et al., 2009), these "key beds" were considered by Sakuma et al. (2012) as further proof that the way up of the MjL section was to the south. Yamakita et al. (2016) revisited the MjL section and found Spathian conodonts from strata believed by conodont and radiolarian workers to be the upper part (Sakuma et al. (2012)'s "lower" part) and insisted that the stratigraphic way up adopted by conodont and radiolarian studies were correct. While Sakuma et al. (2012), being the only internationally "accessible" paper on the stratigraphy of the MjL section, has been cited by international workers (Romano et al., 2013; Thomazo et al. 2016; Hammer et al., 2019; Zhang F. et al. 2019; Zhang L. et al., 2019), Muto et al. (2020) pointed out the serious conflict of Sakuma et al. (2012)'s age model with conodont occurrences.

In this study, we combined new conodont data with that of Yamakita et al. (2010, 2016). The latter two were presented in abstracts from meetings of the Paleontological Society of Japan, and illustrations are made available in this study. The combined data show a stratigraphic distribution of conodonts that is consistent with available works on Early Triassic conodont biostratigraphy (see text for details), when the stratigraphic way up of the conodont and radiolarian workers are accepted. The conodont data is incompatible with the age assignment of the MjL section by Sakuma et al. (2012). To be specific, we found the middle Smithian conodont *Conservatella conservativa* from the "Spathian" interval in Sakuma et al. (2012). In addition, the order of occurrence of *Guangxidella bransoni* and *Scythogondolella milleri* would be reversed from current biostratigraphic schemes if Sakuma et al. (2012)'s age model is to be followed.

We also draw attention to the fact that the reference to conodont occurrences made in the figure of Sakuma et al. (2012) is incorrect. They showed conodont fossil occurrences reported by Takahashi et al. (2009) and Yamakita et al. (2010) on their figures. While correctly explained in their text, the horizons bearing the Smithian conodonts *Guangxidella bransoni* and *Scythogondolella milleri* by Yamakita et al. (2010) are shown the other way around in their figures 5 and 9 (Figs. AP1 and AP2). As explained in the main text, the late Smithian *S. milleri* is known to occur above the middle Smithian *G. bransoni*. By misplacing the conodont occurrences, figures 5 and 9 of Sakuma et al. (2012) seems as if their age model for the MjL section is in accordance with conodont

biostratigraphic schemes. In addition, the horizons bearing the Spathian conodont "*Neospathodus symmetricus*" in Takahashi et al. (2009) are also shown erroneously in Sakuma et al. (2012) (Figs. AP1 and AP2). When the conodont occurrences in the MjL and MjU sections are plotted correctly on the figures of Sakuma et al. (2012), it is evident that their age model for the MjL section is at odds with conodont data (Figs. AP1 and AP2): their model brings the occurrence of middle Smithian conodonts *C. conservatella* and *G. bransoni* above that of the late Smithian conodont *S. milleri*, and also assumes that the beds bearing *C. conservatella* is equivalent to beds bearing the Spathian conodont "*N. symmetricus*". Note also that the "key beds" on which they based the latter interpretation are not uncommon in Lower Triassic deep-sea claystone-dominant facies (e.g., Muto, 2021), and is not a good indicator for locating stratigraphically equivalent beds.

Finally, the inferences of the stratigraphic way up made from sedimentary microstructures by Sakuma et al. (2012) are indecisive. Sakuma et al. (2012) determined the way up of strata based on two features. Firstly, they identified burrows filled with black claystone in a grey claystone bed, which they interpreted to be introduced from the "overlying" black claystone bed (Fig. AP3; Figure 7b of Sakuma et al., 2012). However, the burrows are not connected to the "overlying" black claystone bed. Therefore, the black claystone in the burrows may result from abundant organic matter derived from the burrowers, rather than a result of mechanical transport from the "overlying" black claystone bed. Secondly, Sakuma et al. (2012) identified black claystone beds with a sharp "base" and a gradual "top" (Fig. AP3; Figure 7a of Sakuma et al., 2012). The sharp "base" was interpreted to represent a cessation of bioturbation due to anoxic conditions in the black claystone, while the gradual "top" was interpreted as a result of bioturbation that occurred when anoxic conditions ceased. Fortunately, Sakuma (2010MS, PhD Thesis) provided high-resolution description of the lithology and ichnofabric of the Momotaro-Jinja section along with scanned images and soft X-ray radiographs of slab samples, which allow the reassessment of the interpretation by Sakuma et al. (2012). The interpretation by Sakuma et al. (2012) would be substantiated if the black claystone beds with a sharp "base" is laminated and the gradual "top" of the black claystone beds and the gray-colored bed "above" it are bioturbated (Fig. AP4). However, none of the 27 black claystone beds in the section fit this pattern (Appendix Figure AP4). On the contrary, well-preserved lamination above the gradual "top" of black claystone beds in three horizons indicates that the gradual "top" of the black claystone beds are not necessarily

formed by bioturbation during the deposition of the “overlying” gray beds. Hence, the stratigraphic way up interpreted from the black claystone beds in Sakuma et al. (2012) is indecisive. Consequently, the conodont-based stratigraphic way up and age of the MjL section can be safely adopted.

Regarding the MjU section, Kuwahara and Yao (1997) recognized the *Pa. nakatsugawaensis* and *Hz. gifuensis* zones and correlated the boundary of the two zones to the Lower–Middle Triassic boundary, as explained above. This age assignment was followed by subsequent works (Takahashi et al., 2009, 2015; Ikeda et al., 2010; Sakuma et al., 2012). However, *Hz. gifuensis*, the marker species of this zone was not found from the Momotaro-Jinja section and its lateral extent (Section T of Sugiyama, 1997). Based on cooccurrence with conodonts, Muto et al. (2019) revised the age assignment of radiolarian biozones and concluded that the entire MjU section is of Spathian age.

References

Hammer, Ø., Jones, M.T., Schneebeli-Hermann, E., Hansen, B.B., Bucher, H., 2019. Are Early Triassic extinction events associated with mercury anomalies? A reassessment of the Smithian/Spathian boundary extinction. Earth-Science Rev. 195, 179–190. https://doi.org/10.1016/j.earscirev.2019.04.016

Ikeda, M., Tada, R., Sakuma, H., 2010. Astronomical cycle origin of bedded chert: A middle Triassic bedded chert sequence, Inuyama, Japan. Earth Planet. Sci. Lett. 297, 369–378. https://doi.org/10.1016/j.epsl.2010.06.027

Ikeda, M., Tada, R., 2014. A 70 million year astronomical time scale for the deep-sea bedded chert sequence (Inuyama, Japan): Implications for Triassic-Jurassic geochronology. Earth Planet. Sci. Lett. 399, 30–43. https://doi.org/10.1016/j.epsl.2014.04.031.

Muto, S., 2021. Recurrent deposition of organic-rich sediments in Early Triassic pelagic Panthalassa and its relationship with global oceanic anoxia: New data from Kyoto, Southwest Japan. Glob. Planet. Change 197, 103402. https://doi.org/10.1016/j.gloplacha.2020.103402

Romano, C., Goudemand, N., Vennemann, T.W., Ware, D., Schneebeli-Hermann, E., Hochuli, P.A., Brühwiler, T., Brinkmann, W., Bucher, H., 2013. Climatic and biotic

upheavals following the end-Permian mass extinction. Nat. Geosci. 6, 57–60. https://doi.org/10.1038/ngeo1667

Sakuma, H., Tada, R., Ikeda, M., Kashiyama, Y., Ohkouchi, N., Ogawa, N.O., Watanabe, S., Tajika, E., Yamamoto, S., 2012. High-resolution lithostratigraphy and organic carbon isotope stratigraphy of the Lower Triassic pelagic sequence in central Japan. Isl. Arc 21, 79–100. https://doi:10.1111/j.1440-1738.2012.00809.x

Sakuma, H., 2010MS. High-resolution reconstruction of the deep-water environment and its relation with shallow-water environment during the end-Permian to the Early Triassic: Implication for the case and consequence of ocean anoxia at the P/T boundary. PhD Thesis, Univ. Tokyo.

Sugiyama, K., 1997. Triassic and Lower Jurassic radiolarian biostratigraphy in the siliceous claystone and bedded chert units of the southeastern Mino Terrane, Central Japan. Bull. Mizunami Fossil Museum, 24, 79–193.

Takahashi, S., Oba, M., Kaiho, K., Yamakita, S., Sakata, S., 2009a. Panthalassic oceanic anoxia at the end of the Early Triassic: A cause of delay in the recovery of life after the end-Permian mass extinction. Palaeogeogr. Palaeoclimatol. Palaeoecol. 274, 185–195. https://doi:10.1016/j.palaeo.2009.01.010

Thomazo, C., Brayard, A., Elmeknassi, S., Vennin, E., Olivier, N., Caravaca, G., Escarguel, G., Fara, E., Bylund, K.G., Jenks, J.F., Stephen, D.A., Killingsworth, B., Sansjofre, P., Cartigny, P., 2018. Multiple sulfur isotope signals associated with the late Smithian event and the Smithian/Spathian boundary. Earth-Science Rev. 0–1. https://doi.org/10.1016/j.earscirev.2018.06.019

Yao, A., Kuwahara, K., 1997. Radiolarian faunal change from Late Permian to Middle Triassic times. News Osaka Micropalaeontol., Spec. Vol., no. 10, 87–96 (in Japanese with English abstract).

Yamakita, S., Takahashi, S., Kojima, S., 2010. Conodont-based age-determination of siliceous claystone in the lower part of the Momotaro-jinja section, Inuyama, central Japan. In: Abstr. 2010 Annu. Meet. Palaeontol. Soc. Japan, C23, p. 47 (in Japanese).

Yamakita, S., Kaiho, K., Fujibayashi, M., Takahashi, S., Kojima, S., 2016. Smithian/ Spathian boundary in the Lower Triassic ocean-floor sequence of the Momotaro-jinja section, Inuyama, central Japan. In: 2016 Regul. Meet. Palaeontol. Soc. Japan, B13, p.31 (in Japanese).

Zhang, F., Algeo, T.J., Cui, Y., Shen, J., Song, H., Sano, H., Rowe, H.D., Anbar, A.D., 2019. Global-ocean redox variations across the Smithian-Spathian boundary linked to concurrent climatic and biotic changes. Earth-Science Rev. 195, 147–168. https://doi.org/10.1016/j.earscirev.2018.10.012

Zhang, L., Orchard, M.J., Brayard, A., Algeo, T.J., Zhao, L., Chen, Z.-Q., Lyu, Z., 2019. The Smithian/Spathian boundary (late Early Triassic): A review of ammonoid, conodont, and carbon-isotopic criteria. Earth-Science Rev. 195, 7–36. https://doi.org/10.1016/j.earscirev.2019.02.014

Figure explanations

Figure AP1：Geologic map of Momotaro-Jinja section drawn by Sakuma et al. (2012). Localities of conodont fossils reported by this study and Yamakita et al. (2010) are shown on the map.

Figure AP2：Columnar sections in Momotaro-Jinja section drawn by Sakuma et al. (2012). The horizons of conodont fossil occurrences reported by this study and Yamakita et al. (2010) are corrected and shown in red-colored texts on the figure. Sakuma et al. (2012) cite Yamakita et al. (2010) and use their conodont data, but the horizons of *Scythogondolella milleri* and *Guangxidella bransoni* have been placed the other way around. After our correction, the horizons that were used to correlate the MjL and MjU sections in Sakuma et al. (2012), the “uppermost” part of MT-3 and the lowermost part of MT-4 therein, belong to the middle to lower parts of the Smithian and within the Spathian, respectively. The two belong to completely different substages and cannot be correlated. Because of these facts, the correlation between MjL (MT-3) and MjU (MT-4) by Sakuma et al. (2012) is unacceptable.

Figure AP3：

Photographs of a polished specimen (vertical cross section) of gray siliceous claystone bed and black claystone interbed described in Sakuma et al. (2012). They argued that

194 dark-colored patches in the “Gray Shale Unit” are borrow structures excavated from
195 “Upper Black Shale”. However, these are not connected to the “overlying” black
196 claystone.
197

198 **Figure AP4：**

199 Re-examination of the sedimentological evidence used by Sakuma et al. (2012) to
200 determine the way up of strata in the Momotaro-Jinja-section. The ichnofabric data
201 presented in Sakuma (2010MS) cannot prove that the sharp contact of black claystone
202 with grey claystone is its base. Hence, the way up of strata adopted by Sakuma et al.
203 (2012) is not conclusive.
204
205
206
207
208

Figure AP1

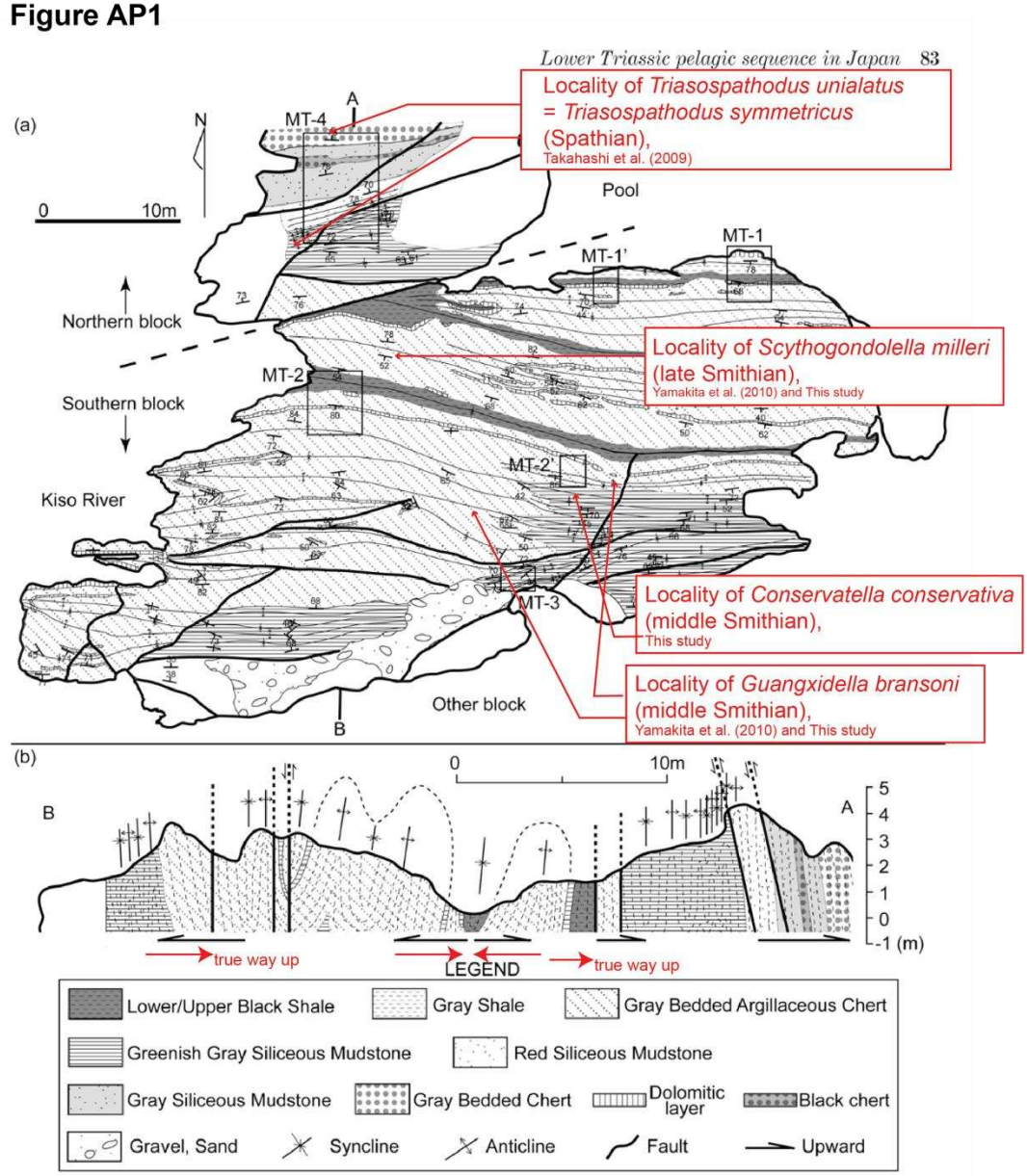

Fig. 3 (a) Geologic sketch map with locations of the six sections (rectangles) (MT-1, -1′, -2, -2′, -3, and -4), and (b) cross-sectional profile of the mapped area near Momotaro Shrine.

209

Figure AP2

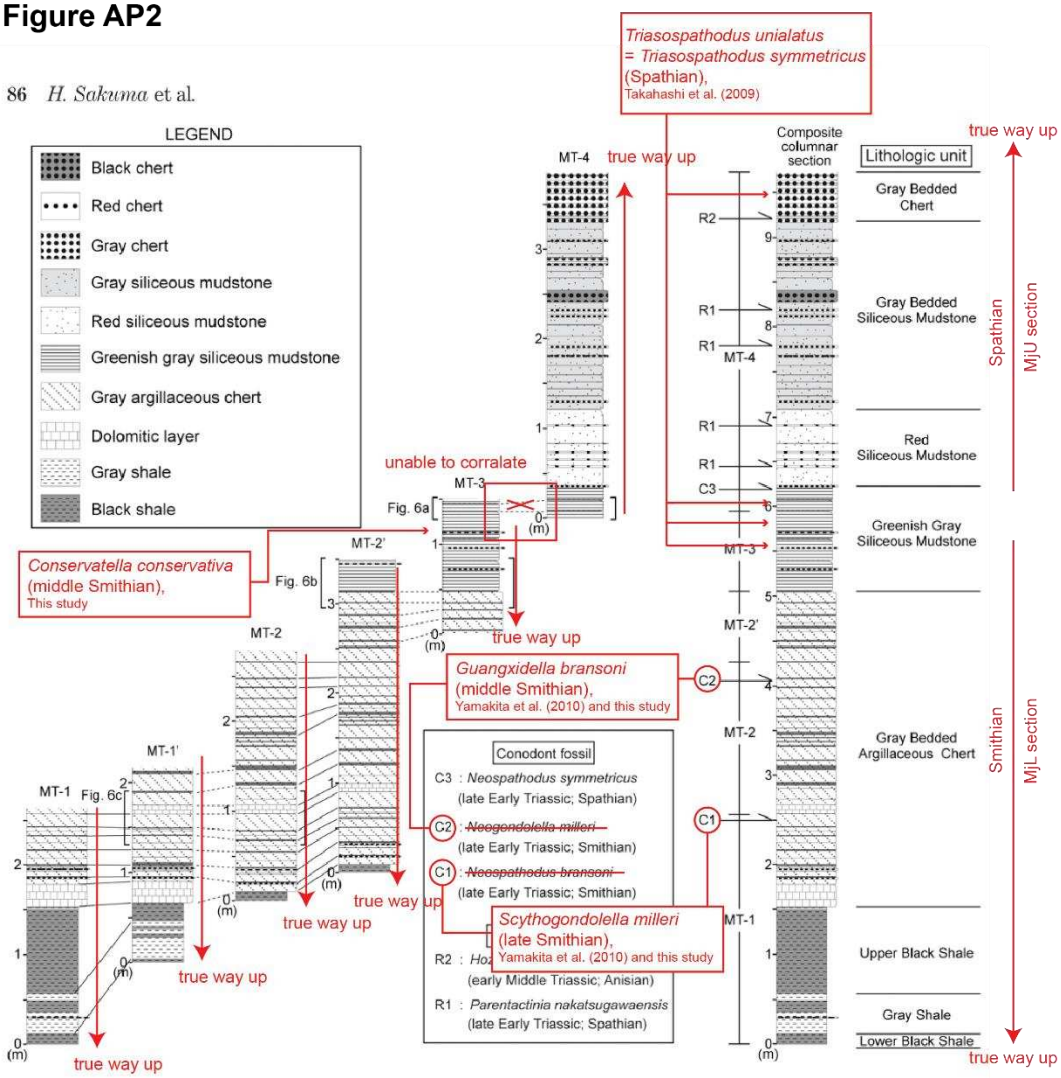

Fig. 5 Correlation of columnar sections at Inuyama section. Solid and dotted lines that correlate columnar sections represent direct and indirect lithostratigraphic correlations, respectively. Arrows indicate horizons that age diagnostic conodont fossils and radiolarian zones have been reported (Yao & Kuwahara 1997; Takahashi *et al.* 2009b; Yamakita *et al.* 2010). Lithostratigraphically correlated intervals at Inuyama section shown in Figure 6 are also indicated on the left or right side of the column. The continuous composite columnar section is shown to the right of the figure.

210

211

Figure AP3

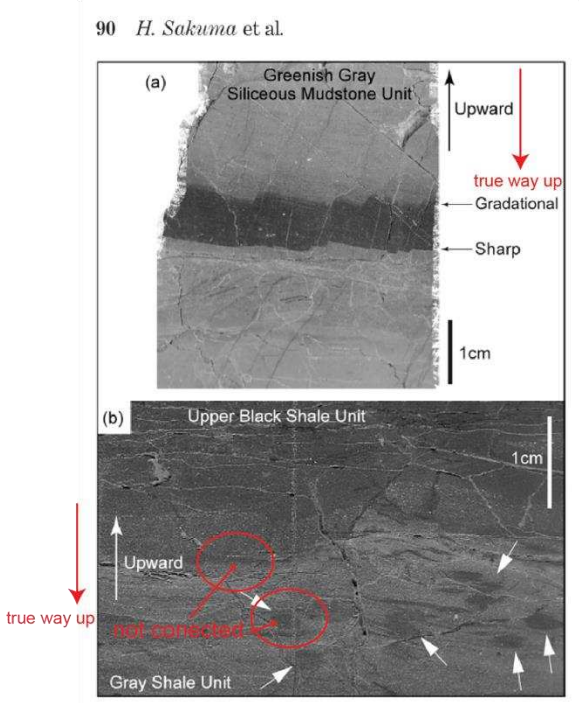

Fig. 7 (a) Stratigraphic direction inferred from the sharp lower and the gradual upper contacts of a thin black shale bed. Color grading around the thin black shale bed is considered to reflect change in concentrations of organic material. Sharp lower contact corresponds to the boundary of depositional environments from oxygen-rich to oxygen-deficient, representing the lack of bioturbation. On the other hand, gradual upper contact corresponds to the boundary of depositional environment from oxygen-deficient to oxygen-rich, representing the influence of bioturbation. Sample was taken from the Greenish Gray Siliceous Mudstone Unit in section MT-3. (b) Stratigraphic direction inferred from black shale filled burrows in gray shale near the boundary between the Gray Shale Unit and the Upper Black Shale Unit in section MT-1. Burrows are indicated by arrows.

212

213

Figure AP4

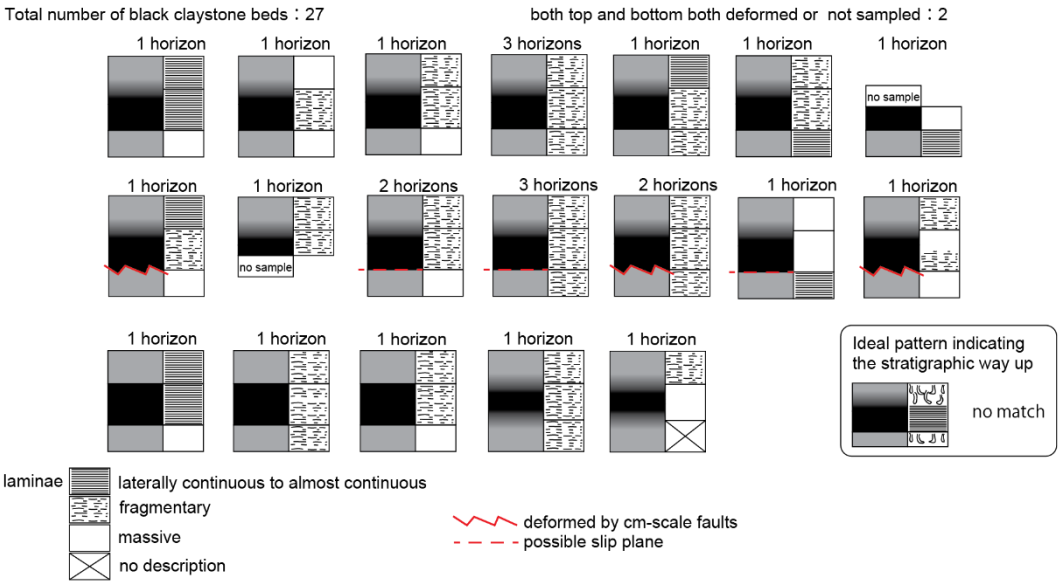
Total number of black claystone beds：27
both top and bottom both deformed or not sampled：2
1 horizon
1 horizon
1 horizon
3 horizons
1 horizon
1 horizon
1 horizon
no sample
1 horizon
1 horizon
no sample
2 horizons
3 horizons
2 horizons
1 horizon
1 horizon
1 horizon
1 horizon
1 horizon
1 horizon
1 horizon
Ideal pattern indicating the stratigraphic way up
no match
laminae
laterally continuous to almost continuous
fragmentary
massive
no description
deformed by cm-scale faults
possible slip plane